J. Fluid Mech. (1988), *vol.* 195, *pp.* 113–135
Printed in Great Britain

Sound generated from the interruption of a steady flow by a supersonically moving aerofoil

By J. E. FFOWCS WILLIAMS AND Y. P. GUO
Department of Engineering, University of Cambridge, Trumpington Street, Cambridge CB2 1PZ, UK

(Received 10 August 1987)

This paper examines a flow–aerofoil interaction problem that we believe is likely to be an important issue in advanced aircraft propulsion systems involving supersonic propellers. They are potentially noisy and it is important to identify the mechanism by which they generate noise so that they can be optimized for acceptable operation. One of the most potent sources of noise lies in the possibility that a second stage propeller blade cuts through the core of the tip vortex shed from a first stage blade. Then suddenly the streaming core flow must adjust to the boundary constraints of that second stage blade, and the adjustment will inevitably involve compressive waves that escape as sound. How strong these sound waves are, how long their life is and where they go to are important questions, the answers to some of which are obtained in this paper. We examine here what we think is a canonical problem and determine the level and directionality of the sound generated by the interruption of the axial vortex-core flow by a supersonic blade. The principal sound is launched in the Mach-wave direction, where the pressure pulse has an amplitude that decreases much more slowly than it would from spherical spreading. This pressure pulse can reach a distant observer with a very large amplitude, 160 dB or higher being typical. The peak sound pressures are found to be independent of blade speed at high supersonic tip velocity, while the energy radiated in the pulse, because of its reducing duration, attenuates as the supersonic speed increases. This aspect gives grounds for believing that the higher the speed, the quieter will be the stage interaction sound of a contrarotating supersonic propeller.

1. Introduction

Pressures on fuel economy and high flight speed lead to the prospect of multistage multibladed propellers whose tips move through the flow with supersonic speed (see figure 1). This is a potentially noisy prospect, and the most intense sound is likely to come from the unsteady conditions created when an aerofoil crosses quickly through the vortical tip flow of the previous propeller stage (figure 2). This intense interaction is not only likely to be the noisiest source but it is also most difficult to analyse and quantify. Analysis is difficult because the flow is nonlinear, and experiments are not easy because rigs need high power and precision – not to mention the safety aspects. It is therefore appropriate to consider approximate models, models that can perhaps contain essential features of the complicated complete problem while being simple enough to analyse exactly. It would be very useful to solve a canonical problem and that is what this paper is about.

Efficient supersonic aerofoil sections are likely to work at low angles of incidence and to conform with linearized inviscid supersonic aerodynamics. The interactions of

FIGURE 1. A high-speed propeller producing a vortex-tip flow behind it.

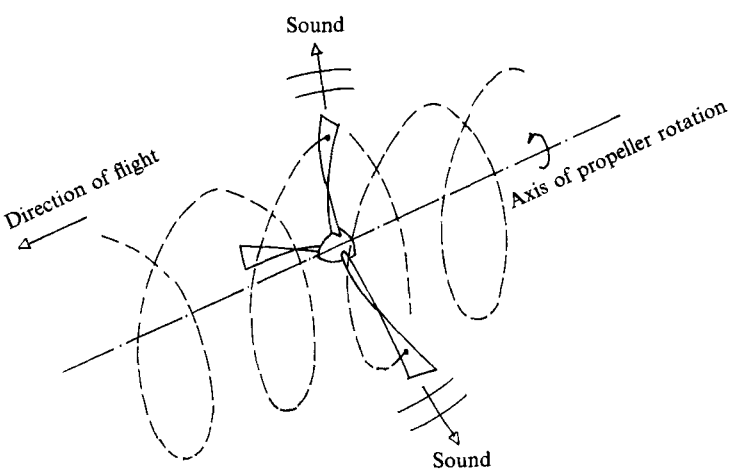

FIGURE 2. Sound is generated by the interruption of the vortex tip flow from the first stage propeller by the second stage propeller.

such an aerofoil with a wake flow might also be analysed in the first instance according to linear theory, whereupon the sound-producing interaction is an effect to be added linearly to the basically steady blade motion. The sound generated by that interaction can then be computed in the simpler case where the aerofoil moves without a steady load. If we neglect the linearly additional effects of blade thickness, our problem then reduces to the sound of a zero-thickness flat aerofoil moving supersonically and inviscidly in its own plane, producing sound as it crosses an inhomogeneity of the flow. The sound so generated is likely to contain sharp-fronted weak shock waves and as such will propagate relative to and through the inhomogeneous propulsion stream according to 'ray theory'. The sound of the

leading edge will not be overtaken by that from the trailing edge of the propeller blade in the most noisy 'Mach-wave' direction, so that the sound generation problem is essentially modellable by treating the leading edge as the edge of a semi-infinite flat plate. Of course, this is an enormously simplified model of the practical case, but it does, we think, contain a basic for calculating rigorously the strength of the most intense pressure pulse that will be generated by a supersonically moving blade impacting an inhomogeneity of the flow. The manner in which this sound reaches the distant observer, depending as it does on the refraction influences of those parts of the propulsion flow through which it travels, can only be determined when those influences are themselves properly modelled. To attempt both the generation and propagation problem at the same time is, we think, an unreasonably challenging task, which we are happy to put off until later.

The structure of the inhomogeneity which is to be scattered into sound by the supersonic aerofoil is also complicated enough to merit a gentle approach through a tractable idealized case. The main disturbance we are contemplating is the tip-vortex flow spreading downstream of the tip of the leading propeller blade. That vortex core, of course, moves with the main flow so that it lies at rest if we fix our coordinate axes in the flow, and the scattering aerofoil moves through it at small incidence with constant speed. Now it can happen that the aerofoil 'chops' the trailing vortex without disturbing the flow circulating about the vortex, the circular streamlines being in the plane of blade motion. In fact, we think that this may be a desirable design objective. But the inevitable axial vortex-core flow cannot lie parallel to the aerofoil, and so it will be interrupted by blade passage, interrupted normally in the situation we perceive. That impact will generate sound, and it is our purpose here to quantify its magnitude and general characteristics.

These supersonic propellers will operate at very high Reynolds number, the main features of such flows being unaffected by viscosity, and being therefore loss-less. The flow at the centre of the vortex system, a tightly rolled multiply layered vortex sheet in which the flow is largely irrotational, will have the same steady-flow pressure–velocity relationship as would a purely irrotational flow. The pressure in the vortex core will be equal to that at its boundary, so therefore will be its velocity, but this time the velocity will lie in an axial direction. We expect there to be an axial velocity field in the vortex core of the same order of magnitude as the circulatory field that surrounds the vortex; of the same order as the propeller-tip speed. This, when interrupted by a supersonically moving aerofoil, will inevitably be noisy. The simplest possible model containing the essential features of this vortex–blade interaction problem is, we think, a supersonic aerofoil that moves in its own plane perpendicular to a uniform cylindrical flow (the vortex core), and in this paper we examine in detail the sound generated by this interaction.

The unsteady field set up by thin aerofoils moving through a non-uniform flow is by no means a new problem. It has been thoroughly studied over the last fifty years (see, for example, von Kármán & Sears 1938; Temple 1953; Ward 1955; Miles 1959) because of its relevance to the gust loading of aircraft wings. The techniques used to determine the unsteady wing loading are the same as those needed to characterize the sound field that radiates away from the aerofoil, though that is an aspect which is not covered in the classical gust-loading literature. The concern with noise is relatively recent and the prospect of counter-rotating supersonic propellers is very new indeed, and this gives rise to the need now to explore aspects of the classical gust problem that were previously irrelevant. Amiet (1986*a*, *b*) has described the subsonic aerofoil–flow interaction problem and our concern is to add to the general body of

knowledge by solving the supersonic problem. In doing so, we find interesting energetic relations between the steady flow and sound field and very considerable structure in the field scattered by supersonically moving aerofoils.

2. Sound generated by a semi-infinite aerofoil

We consider a semi-infinite aerofoil moving supersonically in its own plane perpendicular to a uniform cylindrical flow of radius a. The coordinates system is chosen in such a way that the aerofoil lies in the plane $x_3 = 0$, with its leading edge being parallel to the x_2 axis and advancing at speed cM, c being the constant sound speed and the Mach number M being larger than unity. The leading edge of the aerofoil coincides with the x_2 axis at time $t = 0$. The cylindrical flow has a uniform velocity u_0 in the negative-x_3 direction, and its axis is chosen to be the x_3 axis. The situation is illustrated in figure 3. We consider the sound generated linearly by the interruption of the uniform cylindrical flow by the moving aerofoil. The total flow field can then be regarded as the linear superposition of the cylindrical flow and an induced disturbance velocity field u_i. Owing to the symmetrical geometry, it is sufficient to consider only the region $x_3 \geqslant 0$. The sound pressure can be conveniently calculated through the use of Kirchhoff's theorem (Dowling & Ffowcs Williams 1983), which relates the acoustic pressure at any observation position to the velocity distribution on the plane $x_3 = 0$, namely,

$$p(\boldsymbol{x}, t) = \frac{\rho_0}{2\pi} \frac{\partial}{\partial t} \int_{y_\alpha} \left[\frac{u_3(\boldsymbol{y}, \tau)}{|\boldsymbol{y}-\boldsymbol{x}|}\right] \mathrm{d}^2 y_\alpha, \tag{2.1}$$

where ρ_0 is the constant mean density, u_3 denotes the x_3 component of the induced velocity field u_i and the square brackets have the conventional retarded time implication, the quantity enclosed being evaluated at the retarded time $\tau = t - |\boldsymbol{y}-\boldsymbol{x}|/c$. The integrand of (2.1) is to be evaluated at $y_3 = 0$, where the distribution of u_3 can be specified as

$$u_3(\boldsymbol{y}, \tau) = u_0 H(a^2 - y_\alpha^2)\, H(cMt - M|\boldsymbol{y}-\boldsymbol{x}| - y_1), \tag{2.2}$$

where H is the Heaviside step function, equal to unity for positive arguments and zero for negative arguments. This specification follows from the fact that the induced velocity vanishes ahead of the leading edge of the aerofoil, because the leading edge moves faster than sound, while on the aerofoil surface it also vanishes except in the region covered by the cylindrical flow, where it must be opposite to the flow velocity, to comply with the boundary condition that the total normal velocity on the aerofoil surface is zero. On substituting (2.2) into (2.1) and carrying out the partial derivative with respect to time t by noticing that the gradient of the Heaviside function is the Dirac delta function, we find that

$$p(\boldsymbol{x}, t) = \frac{\rho_0 u_0 cM}{2\pi} \int_{y_\alpha} \frac{1}{|\boldsymbol{y}-\boldsymbol{x}|} H(a^2 - y_\alpha^2)\, \delta(cMt - M|\boldsymbol{y}-\boldsymbol{x}| - y_1)\, \mathrm{d}^2 y_\alpha. \tag{2.3}$$

The δ-function can be utilized to evaluate the y_2 integral. The method of doing it can be found in books on generalized functions (e.g. Jones 1982). When this is done, we find that

$$p(\boldsymbol{x}, t) = \frac{\rho_0 u_0 c}{2\pi} \int_{y_1} \frac{H(a^2 - y_1^2 - y_+^2) + H(a^2 - y_1^2 - y_-^2)}{\{(y_1 - cMt)^2 - M^2[(y_1 - x_1)^2 + x_3^2]\}^{\frac{1}{2}}} \times H(cMt - y_1)\, H[(y_1 - cMt)^2 - M^2[(x_1 - y_1)^2 + x_3^2]]\, \mathrm{d}y_1, \tag{2.4}$$

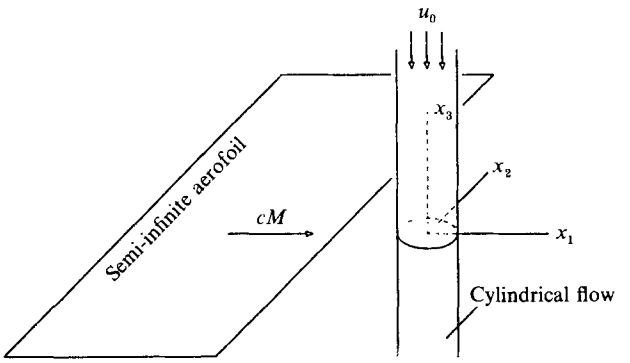

FIGURE 3. The geometry and the coordinate system of the model problem. The spherical coordinates (r, ϕ, θ) used in the text and the subsequent figures are defined by $x_1 = r\sin\theta\cos\phi$, $x_2 = r\sin\theta\sin\phi$ and $x_3 = r\cos\theta$.

where $y_\pm$ are determined by solving the equation $cMt - M|\boldsymbol{y}-\boldsymbol{x}| - y_1 = 0$ for y_2, that is,

$$y_\pm = x_2 \pm \frac{1}{M}\{(y_1 - cMt)^2 - M^2[(y_1-x_1)^2 + x_3^2]\}^{\frac{1}{2}}. \tag{2.5}$$

The determination of $y_\pm$ also results in the last two Heaviside functions in (2.4); when either of the arguments of the two is negative, $cMt - M|\boldsymbol{y}-\boldsymbol{x}| - y_1 = 0$ has no real solution for y_2, and hence the integral vanishes. Now, it can be recognized that (2.4) can be integrated to inverse sine functions (e.g. Gradshteyn & Ryzhik 1980, formula 2.261),

$$p(\boldsymbol{x}, t) = \frac{\rho_0 u_0 cM}{2\pi(M^2-1)^{\frac{1}{2}}} \arcsin \frac{(M^2-1)y_1 - M(Mx_1 - ct)}{M[(x_1 - cMt)^2 - (M^2-1)x_3^2]^{\frac{1}{2}}}\Bigg|_A^B, \tag{2.6}$$

the integration bounds A and B being determined by the Heaviside functions in the integrand of (2.4). In doing so, quartic equations arising from the vanishing of the arguments of the Heaviside functions must be solved, which is algebraically complicated and tedious, except in the case of $x_2 = 0$ which we will examine in the next section. It is straightforward, however, to solve these equations numerically. The sound pressure can then be obtained according to (2.6).

Plotted in figure 4 is the sound pressure as a function of the radial position r in the direction $\phi = \theta = \frac{1}{4}\pi$, where (r, ϕ, θ) are the spherical coordinates defined by

$$x_1 = r\sin\theta\cos\phi, \quad x_2 = r\sin\theta\sin\phi, \quad x_3 = r\cos\theta.$$

This figure is representative of any direction other than that along the Mach angle, which will be discussed shortly. Apparently, the sound is generated in the form of a pressure pulse that is switched on and off at zero amplitude. The maximum amplitude occurs in the middle of the pulse. As time increases, the waveform propagates away at constant speed c with its maximum amplitude decreasing according to $1/r$, or, equivalently $1/ct$, obviously owing to spherical spreading, which is illustrated in figure 4 by the dashed curve. The pressure *vs.* radius curves are all smooth and rounded in the far field, but have sharp faces in the near field (the curves corresponding to $cMt/a = 2.0$ and 4.0) when the leading edge of the aerofoil is within the cylindrical flow, because the pressure perturbations in this case jump from zero to a constant value across the edge of the Mach cone from the leading edge. As time t increases, the initial rectangular pressure form travels to the far field with its height

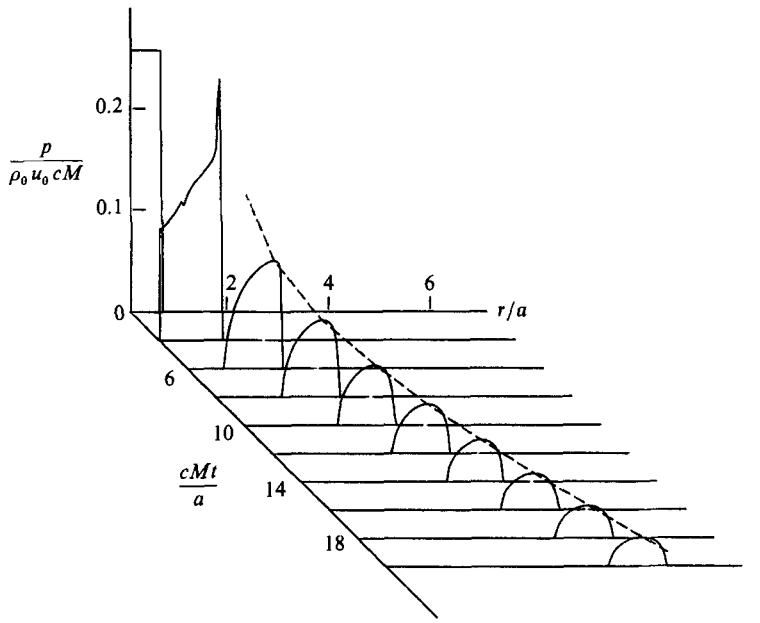

FIGURE 4. Sound pressure calculated according to (2.6) with $M = 4.0$ in the direction $\phi = \theta = \frac{1}{4}\pi$. The $1/r$ decrease is illustrated by the dashed curve.

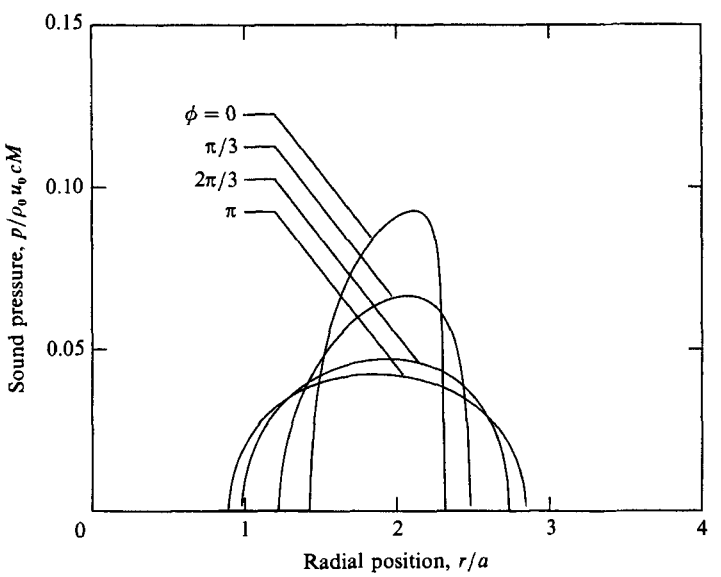

FIGURE 5. The angular distribution in the ϕ-direction of the sound pressure for $\theta = \frac{1}{4}\pi$, $cMt/a = 8.0$ and $M = 4.0$.

decreasing owing to spherical spreading. That decrease starts at the rear face of the pressure pulse, so that, when $cMt/a = 4.0$, only a very narrow part close to the front face of the initial rectangular waveform still remains its initial height, while most of the pulse has greatly decreased in amplitude. This gives the peak (of finite height) in the second curve at $cMt/a = 4.0$ in figure 4.

To demonstrate the directionality of the generated sound we calculate, and depict in figures 5 and 6, the sound pressures in different directions. In the far field $r/a \gg 1$,

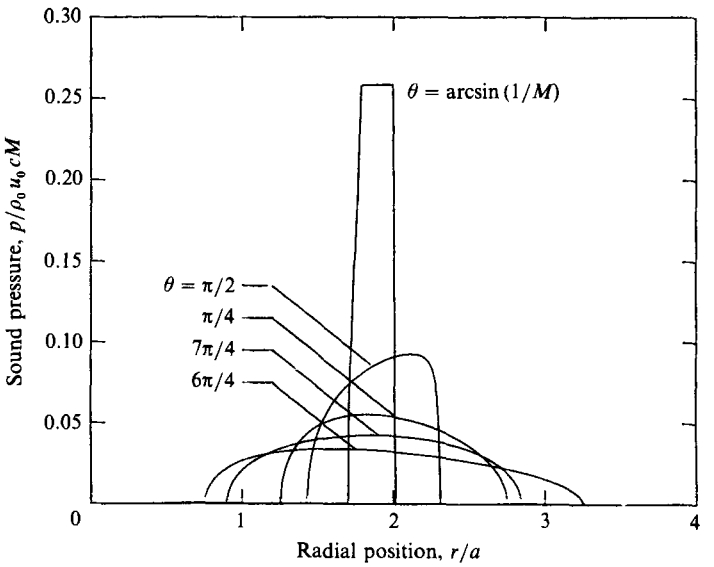

FIGURE 6. The angular distribution in the θ-direction of the sound pressure for $\phi = 0$, $cMt/a = 8.0$ and $M = 4.0$.

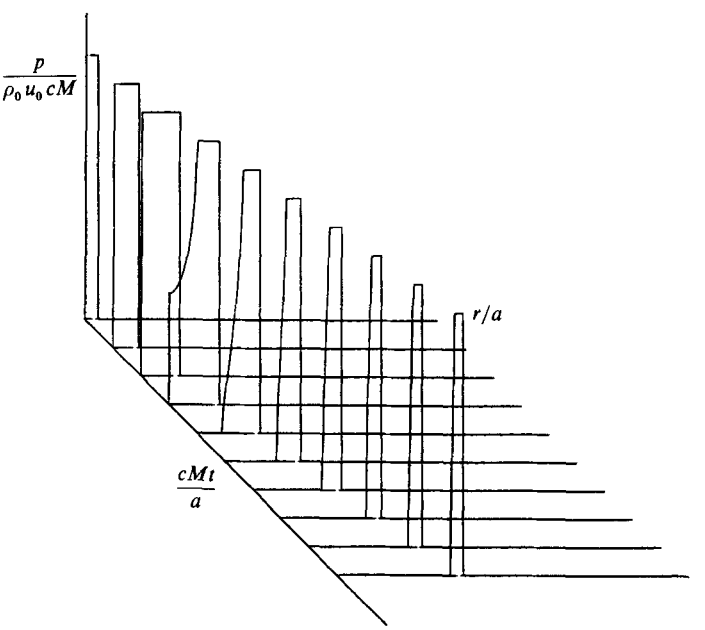

FIGURE 7. A constant pressure pulse is launched in the Mach-wave direction $\phi = 0$ and $\theta = \arcsin(1/M)$. The time increment in the figure is 1.0 and the magnitude of the pulse is $1/(M^2-1)^{\frac{1}{2}}$.

sound pressures usually decrease as $1/r$ owing to spherical spreading. However, it is evident that the amplitude of the pressure pulse is unaffected by the spherical spreading in the Mach-wave direction dead ahead of the moving aerofoil, that is, in the direction of $\phi = 0$ and $\sin\theta = 1/M$. This indicates that a pressure pulse of constant amplitude is launched in this direction. This situation is shown in figure 7. It is clear that a sharp-fronted pulse is generated by the impact on the flow of the

moving aerofoil. This pressure pulse propagates along the Mach-wave direction at speed c without attenuation. The rear face of the waveform also becomes sharp as it travels away. An intense bang will be heard by distant observers in this Mach-wave direction.

All these features can also be derived by calculating the far-field sound from (2.3) through the expansion of the retarded time in the δ-function. Since the source processes are confined to the disk $|y_\alpha| < a$, the quantity $|y_\alpha|/|\boldsymbol{x}|$ is at most of the order $a/|\boldsymbol{x}|$ which is small in the far field. Hence, we have the expansion

$$|\boldsymbol{y}-\boldsymbol{x}| = |\boldsymbol{x}|\left[1-\hat{x}_\alpha\frac{y_\alpha}{|\boldsymbol{x}|}+\frac{1}{2}\frac{y_\alpha}{|\boldsymbol{x}|}\left(\frac{y_\alpha}{|\boldsymbol{x}|}-\hat{x}_\alpha\hat{x}_\beta\frac{y_\beta}{|\boldsymbol{x}|}\right)+O\left(\frac{a^3}{|\boldsymbol{x}|^3}\right)\right], \tag{2.7}$$

where we have set $y_3 = 0$ on the right-hand side and $\hat{x}_\alpha = x_\alpha/|\boldsymbol{x}|\,(\alpha = 1, 2)$ is of order one. In the far field, $|\boldsymbol{x}|/a \gg 1$, the expansion can be truncated after the term proportional to $y_\alpha/|\boldsymbol{x}|$ as the first-order approximation. In this case, the argument of the δ-function in (2.3) becomes

$$M(ct-|\boldsymbol{x}|)-y_1(1-M\hat{x}_1)+M\hat{x}_2 y_2. \tag{2.8}$$

With this simplification, the y_α integral in (2.3) can be evaluated in a straightforward manner. After some simple algebra, we find the far-field solution as

$$p(\boldsymbol{x},t) = \frac{\rho_0 u_0 cM}{\pi\kappa}\left[1-\left(\frac{M\epsilon_2}{\epsilon_1}\right)^2\right]^{\frac{1}{2}}\frac{a}{|\boldsymbol{x}|}, \tag{2.9}$$

where the quantities κ, ϵ_1 and ϵ_2 are defined, to save writing, as

$$\kappa = [M^2\hat{x}_2^2+(1-M\hat{x}_1)^2]^{\frac{1}{2}}, \tag{2.10}$$

$$\epsilon_1 = \frac{a}{|\boldsymbol{x}|\,\kappa}, \quad \epsilon_2 = \frac{ct-|\boldsymbol{x}|}{|\boldsymbol{x}|\,\kappa^2}. \tag{2.11}$$

The far-field behaviour of the generated sound is now clear from (2.9). The sound reaches the far field in the form of a pressure pulse whose shape is characterized by the quantity enclosed in the square root. At the boundaries of the waveform, this quantity vanishes, the pressure pulse being switched on and off at zero amplitude, while in the middle of the waveform, it takes its maximum value of unity. The $1/|\boldsymbol{x}|$ decrease owing to spherical spreading is also evident in (2.9).

When both $\hat{x}_2 = 0$ and $1-M\hat{x}_1 = 0$, that is, in the Mach-wave direction, we notice that κ vanishes so that (2.9) has a singularity, which is a failure of the first-order approximation. The reason for this is that the approximation ignores any variations in the emission time of the finite source distribution; for an observer in the Mach-wave direction, the sound is generated, in this first-order approximation, as if the source were a concentrated point source of structure $\delta(\tau)$. This is apparent from (2.8), which, in this event, reduces to $M(ct-|\boldsymbol{x}|)$, so that the pressure (2.3) is simply

$$p(\boldsymbol{x},t) = \tfrac{1}{2}\rho_0 u_0 cM\delta\left(1-\frac{ct}{|\boldsymbol{x}|}\right)\frac{a}{|\boldsymbol{x}|},$$

a singular field that results from the crude first-order approximation. To account for the variations of the emission time of the sources, it is necessary to truncate the series (2.7) after the term of order $a^2/|\boldsymbol{x}|^2$, which is the leading term in this case. With this

second-order approximation, it can be shown that the pressure fluctuations in the Mach-wave direction are given by

$$p(\boldsymbol{x},t)=\frac{4\rho_0 u_0 cM}{\pi(M^2-1)^{\frac{1}{2}}}\arcsin\left[(M^2-1)\left(\frac{a^2}{2|\boldsymbol{x}|\,(ct-|\boldsymbol{x}|)}-1\right)\right]^{\frac{1}{2}}.$$

The inverse sine function varies from 0 to $\frac{1}{2}\pi$, and hence there is no singularity present. Also, it can be seen that there is no spherical spreading effect in the Mach-wave direction, as illustrated in figure 7.

3. Solution for the case of $x_2 = 0$

In this section, we examine the sound in the plane $x_2 = 0$. We choose to work with this special case because, on the one hand, its solution can be obtained and analysed exactly in closed form, and on the other hand, the general features of the generated sound can all be clearly revealed by this special situation, including the level and directionality of the most intense sound. Letting x_2 vanish, the squares of $y_\pm$, given by (2.5), are then equal and the two Heaviside functions involving $y_\pm$ in (2.4) are identical. Thus, the integration bounds A and B are respectively equal to the lower and the upper bound of an interval in the y_1 axis, determined by the three inequalities

$$cMt-y_1>0,$$

$$(y_1-cMt)^2-M^2[(y_1-x_1)^2+x_3^2]>0,$$

and

$$a^2-y_1^2-\frac{(y_1-cMt)^2}{M^2}+(y_1-x_1)^2+x_3^2>0.$$

Solving these inequalities to find A and B, and calculating the sound according to (2.6), we find that the acoustic pressures have four different non-zero expressions, each being valid in a different region. Denoting the four by p_1, p_2, p_3 and p_4, we have

$$p_{1,2}=\frac{\rho_0 u_0 cM}{\pi(M^2-1)^{\frac{1}{2}}}\left[\tfrac{1}{2}\pi\pm\arcsin\frac{M^2(Mx_1-ct)\pm(M^2-1)[(M^2+1)x_1^2+x_3^2+a^2-2cMtx_1]^{\frac{1}{2}}}{[(x_1-cMt)^2-(M^2-1)x_3^2]^{\frac{1}{2}}}\right], \tag{3.1}$$

$$p_3=\frac{\rho_0 u_0 cM}{(M^2-1)^{\frac{1}{2}}},\quad p_4=p_1+p_2-p_3. \tag{3.2}$$

The distribution of these values is shown in figure 8. When the cylindrical flow is interrupted by the moving aerofoil, sound is scattered, which spreads spherically to the far field. In the Maeh wave direction, the pressure is given by p_3, a sudden increase from zero to a constant value. This sharp-fronted pressure pulse propagates to the far field without attenuation in amplitude, which confirms the discussions of figure 7 in the previous section and indicates that the noisiest sound is heard by observers dead ahead of the moving aerofoil in the Mach-wave direction. The constant magnitude of the pressure pulse p_3 can be seen to be independent of the aerofoil Mach number M at high supersonic speeds, that is, when $M \gg 1$. Actually, this is also true for the maximum of the amplitude of p_1 and p_2. This peak pressure is likely to be very loud. For example, the axial flow down a vortex will usually exceed 10 m/s, in which case the pressure perturbation at the Mach angle is greater than 160 dB. Of course, this pressure pulse will, in real situations, undertake

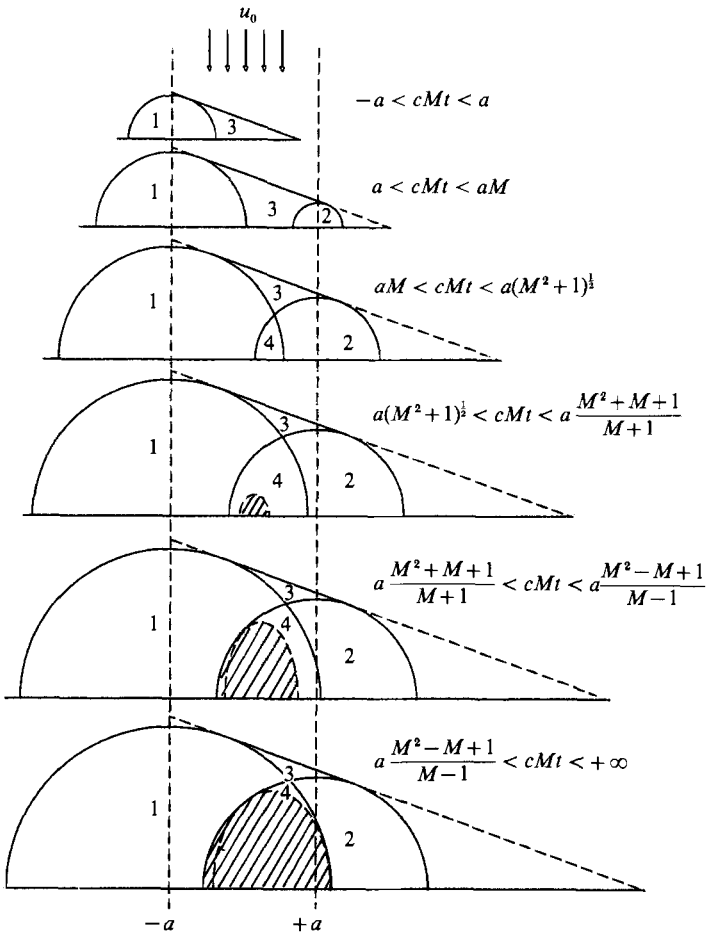

FIGURE 8. The distribution of sound pressure in the plane $x_2 = 0$. The numbers correspond to the subscripts of p in (3.1) and (3.2), e.g. p_1 is the sound in the region labelled 1.

refractive interactions with the inhomogeneous main flow through which the propeller blade moves, and possibly with other blades in a multistage propeller system, before it reaches the far-field observer.

As the aerofoil moves forward, a silent region appears, when $cMt > a(M^2-1)^{\frac{1}{2}}$, near the cylindrical flow, which is indicated by the shadow area in figure 8. The silent region results from the finiteness of the time–space distribution of the source, the scattering process being of finite timescale and occurring within a finite space dimension, which is different from the equivalent two-dimensional problem where the source region is infinite in the y_2 direction. The boundary of the silent area is initially given by the curve

$$\left(x_1 - \frac{cMt}{M^2+1}\right)^2 + \frac{x_3^2}{M^2+1} = \frac{(cMt)^2 - (M^2+1)\,a^2}{(M^2+1)^2}, \tag{3.3}$$

but eventually, when cMt is larger than $a(M^2-M+1)/(M-1)$, it is bounded jointly by the first and the last generated wave, that is, the wave from $x_1 = -a$ and that from $x_1 = a$, and the curve (3.3) as shown in the last diagram of figure 8. Though the small p_4 region shrinks to zero at large t, the curve (3.3) (the dashed curve in

figure 8) never coincides exactly with the waves from $x_1 = -a$ and $x_1 = a$, because some waves propagating in this direction (near the Mach angle) are always behind the first and last generated waves.

As time $t \to +\infty$, the shadow region spreads to the entire space; the whole field becomes silent. Though the pressure fluctuations are then zero, the induced velocity is not, implying that a steady near-field motion is also built up by the impact of the aerofoil and some part of the scattered energy must be trapped near the cylindrical flow. This will be further analysed in the next section.

From the structure of the solutions (3.1) and (3.2), it is evident that the sound pressures are finite everywhere. Near the edge of the Mach cone from the leading edge of the aerofoil, namely, near the Mach line $(x_1 - cMt)^2 - (M^2-1)x_3^2 = 0$, the pressure is given by the constant value p_3. Hence there is no singularity in the pressure field, p_1, p_2 and p_4 being sound in regions not connected with the Mach line.

Solutions (3.1) and (3.2) are exact expressions for the sound field. They can be expanded in the limiting case $r/a \to \infty$ to display explicitly the far-field behaviour of the generated sound. To this end, we use the spherical coordinates (r, ϕ, θ) introduced in the previous section with $\phi = 0$, so that $x_1 = r\sin\theta$ and $x_3 = r\cos\theta$, and denote

$$\kappa = \left[\left(\sin\theta - \frac{cMt}{r}\right)^2 - (M^2-1)\cos^2\theta\right]^{\frac{1}{2}} \tag{3.4}$$

to save writing. The argument of the inverse sine function in (3.1) for p_1 thus becomes

$$\frac{1}{\kappa}\left[M^2\left(M\sin\theta - \frac{ct}{r}\right) + (M^2-1)\left(1 + M^2\sin^2\theta + \frac{a^2}{r^2} - 2M\sin\theta\frac{ct}{r}\right)^{\frac{1}{2}}\right]. \tag{3.5}$$

In this, we can identify two small quantities, namely, a/r and $(ct/r)^2 - 1$. The former is obviously small because we seek solutions for $r/a \to \infty$. The latter can be shown to be small by noticing that p_1 is the sound in a very narrow region bounded by the first and the last generated wave, as shown in figure 8; it is non-zero only if time t is larger than the propagating time of the first generated wave (namely, the wave from $x_1 = -a$), and smaller than that of the last generated wave which comes from $x_1 = a$. Hence, we have

$$\frac{1}{c}(r^2 + a^2 + 2ra\sin\theta)^{\frac{1}{2}} - \frac{a}{cM} < t < \frac{1}{c}(r^2 + a^2 - 2ra\sin\theta)^{\frac{1}{2}} + \frac{a}{cM},$$

from which it can be deduced that

$$-2\frac{a}{r}\left(\frac{1}{M} - \sin\theta\right) < \frac{c^2t^2}{r^2} - 1 < 2\frac{a}{r}\left(\frac{1}{M} - \sin\theta\right), \tag{3.6}$$

to the first order as $a/r \to 0$. Evidently, the maximum order of $(ct/r)^2 - 1$ is usually a/r. Since the narrow region in which p_1 is valid only has one point adjacent to the Mach line, κ is at least of order one except when approaching this line. Therefore, it is convenient and permissible to expand (3.5) in powers of

$$\epsilon_1 = \frac{a}{r\kappa}, \quad \epsilon_2 = \frac{c^2t^2 - r^2}{r^2\kappa^2}. \tag{3.7}$$

It can be noticed that the quantities κ, ϵ_1 and ϵ_2 defined above are actually the first-order terms of (2.10) and (2.11) in the previous section with $x_2 = 0$. In terms of (3.7), the expression (3.5) reduces to

$$-M^2[1-(M^2-1)\,\epsilon_2]^{\frac{1}{2}}+(M^2-1)[1-\epsilon_1^2-M^2\epsilon_2]^{\frac{1}{2}},$$

where the negative sign of the first term comes from the fact that $M\sin\theta - ct/r$ is always negative in the p_1 region. This result can be expanded as

$$-1+\tfrac{1}{2}(M^2-1)\,(\epsilon_1^2-\tfrac{1}{4}M^2\epsilon_2^2)+\ldots, \tag{3.8}$$

where the neglected terms are of higher orders in ϵ_1 and/or ϵ_2. On substituting (3.8) into (3.1), we have

$$p_1 = \frac{\rho_0 u_0 cM}{\pi(M^2-1)^{\frac{1}{2}}}\{\tfrac{1}{2}\pi+\arcsin[-1+\tfrac{1}{2}(M^2-1)\,(\epsilon_1^2-\tfrac{1}{4}M^2\epsilon_2^2)]\}.$$

Noting that $\frac{1}{2}\pi = \arcsin(1)$ and using the formula (1.625) of Gradshteyn & Ryzhik's (1980) book for the addition of inverse sine functions, we find that

$$p_1 = \frac{\rho_0 u_0 cM}{\pi(M^2-1)^{\frac{1}{2}}}\arcsin[(M^2-1)\,(\epsilon_1^2-\tfrac{1}{4}M^2\epsilon_2^2)]^{\frac{1}{2}}.$$

Since the argument inside the square root is very small, we can further expand the inverse sine function to find

$$p_1 = \frac{\rho_0 u_0 cM}{\pi\kappa}\left[1-\left(\frac{M\epsilon_2}{2\epsilon_1}\right)^2\right]^{\frac{1}{2}}\frac{a}{r}. \tag{3.9}$$

Now the physical properties of the far-field sound are clearly revealed. The maximum amplitude of the waves decreases like $1/r$ as $r\to\infty$ owing to spherical spreading. Obviously, this maximum value occurs near the curve $ct = r$, which is in the centre of the waveform, that is, near the wave from the source at the origin. In this case, ϵ_2 tends to zero much more rapidly than ϵ_1, so that (3.9) reduces to

$$p_1 = \frac{\rho_0 u_0 cM}{\pi\kappa}\frac{a}{r}.$$

The $1/r$ decrease is evident. From (3.4), it can be seen that κ is in proportion to M when $M \gg 1$. Thus the maximum amplitude of the sound waves is independent of the aerofoil Mach number M at high supersonic speed. On the other hand, near the boundaries of the p_1 region, we have, from (3.6), that $\epsilon_2 \to 2\epsilon_1/M$, which gives that $p_1 = 0$, consistent with the previous analysis that the pressure pulse in directions other than the Mach-wave direction is switched on and off at zero amplitude. When approaching the Mach line, caution must be used because ϵ_2 must be scaled differently there. From (3.6), it is clear that $(ct/r)^2 - 1$ is in this event smaller than the order a/r, because $\sin\theta \to 1/M$ near the Mach angle. In fact, it can be shown that

$$\frac{c^2t^2}{r^2}-1 \to \frac{M^2-1}{M^2}\frac{a^2}{r^2}.$$

Hence, terms of the order a^2/r^2 in the expansion (3.8) must be retained to find the correct asymptotic solution for this situation. When this is done, we find that the pressure tends to a constant value as it should.

Now, we can derive the far-field approximations for p_2 in the same way. It turns out that p_1 and p_2 have the same asymptotic form as $r/a \to \infty$, which is given by (3.9).

Since p_4 is essentially a linear combination of p_1, p_2 and p_3, it poses no difficulty to analyse its far field. However, it can be noticed that the p_4 region shrinks very rapidly to zero as the pressure waves propagate away. Hence it is sufficient to ignore it as $r \to \infty$. This is evidently reasonable from figure 7; the back face of the waveform rapidly becomes sharp at large t, and the existence of the p_4 region can hardly be noticed.

4. The scattered energy

The sound energy scattered by the moving aerofoil can be found by considering the energy loss of the total flow during the interruption process, that is, by calculating the difference between the energy contained in the flow before the aerofoil cuts the cylindrical flow and that remaining in the field after the interruption process. That energy difference must have escaped to infinity as sound since the dragless aerofoil moves in its own plane and does *no* work. It is evident that the leading edge of the supersonically moving aerofoil does not experience any suction force which could significantly affect the acoustic radiation, as it might do in subsonic situations (Cannell & Ffowcs Williams 1973), because the supersonic leading edge cannot be affected by the disturbances generated by the leading edge itself. It is also evident that no energy is radiated from the aerofoil surface because the energy flux on the plane $x_3 = 0$, in which the aerofoil lies, is identically zero since the total normal velocity on the aerofoil surface ($x_1 < cMt$) always vanishes and the pressure perturbations are always zero ahead of the leading edge ($x_1 > cMt$) that advances at supersonic speed. Hence the total energy (the acoustic and the kinetic energy) in the field is conserved during the whole process of interruption of the steady flow by the semi-infinite aerofoil. The aerofoil generates sound by scattering the jet's energy into sound, the strength of which can be evaluated by energy conservation arguments.

Suppose that the main flow, of velocity $v_i(\boldsymbol{x})$ with $\partial v_i/\partial x_i = 0$, is interrupted by the aerofoil, producing a disturbance velocity potential φ, so that the total velocity of the interrupted flow is $v_i + \partial\varphi/\partial x_i$. In our particular case where the jet flow is perpendicular to the moving aerofoil, v_i only has one component in the negative-x_3 direction (noting that the flow does not have a uniform velocity component in the x_1 direction). At time $t \to -\infty$ when the aerofoil is still far away from the flow v_i, there is no disturbance in the field and the total energy contained in the flow is given by

$$E_{-\infty} = \int \tfrac{1}{2}\rho_0 [v_i(\boldsymbol{x})]^2 \, \mathrm{d}^3\boldsymbol{x}, \tag{4.1}$$

where the volume integral is over the entire space. As time $t \to +\infty$, the leading edge of the semi-infinite aerofoil will move far downstream. The flow is then effectively bounded by an infinite plane boundary at $x_3 = 0$; the interrupted flow will eventually settle down to a steady state with the induced velocity potential determined by the Laplace equation $\nabla^2\phi = 0$ and the boundary condition that the total normal velocity on the aerofoil surface must vanish.

$$\frac{\partial\varphi}{\partial x_3} = -v_3 \quad \text{on } x_3 = 0 \tag{4.2}$$

then imposes the solution for φ (e.g. Jeffreys & Jeffreys 1956)

$$\varphi = \frac{1}{2\pi} \int_{y_\alpha} \frac{v_3(\boldsymbol{y})}{|\boldsymbol{y}-\boldsymbol{x}|} \, \mathrm{d}^2 y_\alpha. \tag{4.3}$$

This is the near-field motion which does not die out with time, so that the total energy remaining in the field at time $t \to +\infty$ is

$$E_{+\infty} = \int \tfrac{1}{2}\rho_0 \left[v_i + \frac{\partial \varphi}{\partial x_i}\right]^2 \mathrm{d}^3\boldsymbol{x}. \tag{4.4}$$

By making use of the relations $\partial v_i/\partial x_i = 0$ and $\nabla^2\varphi = 0$, this can be rewritten as

$$E_{+\infty} = E_{-\infty} + \tfrac{1}{2}\rho_0 \int \frac{\partial}{\partial x_i}\left(2\varphi v_i + \phi \frac{\partial \varphi}{\partial x_i}\right) \mathrm{d}^3\boldsymbol{x}, \tag{4.5}$$

where $E_{-\infty}$ is the energy in the flow at time $t \to -\infty$ and is given by (4.1). The scattered acoustic energy E_a can now be found by calculating the difference between $E_{-\infty}$ and $E_{+\infty}$:

$$E_a = E_{-\infty} - E_{+\infty} = \rho_0 \int_{x_\alpha} \left(2\varphi v_3 + \varphi \frac{\partial \varphi}{\partial x_3}\right) \mathrm{d}^2 x_\alpha, \tag{4.6}$$

where the last step follows from applying the divergence theorem to the volume integral in (4.5). In doing so, we have utilized the symmetrical geometry of the problem and performed the volume integral only in the upper half-space with the result doubled. On the surface of the aerofoil, namely on the plane $x_3 = 0$, we have the boundary condition (4.2). Thus (4.6) can be simplified as

$$E_a = \rho_0 \int_{x_\alpha} \varphi v_3 \, \mathrm{d}^2 x_\alpha.$$

The velocity potential φ is given by (4.3), so that for any initially steady velocity field v_i, the energy scattered into sound by a semi-infinite aerofoil is

$$E_a = \frac{1}{2\pi}\rho_0 \int_{x_\alpha} \int_{y_\alpha} \frac{v_3(\boldsymbol{x})\, v_3(\boldsymbol{y})}{|\boldsymbol{y} - \boldsymbol{x}|} \mathrm{d}^2 x_\alpha \, \mathrm{d}^2 y_\alpha. \tag{4.7}$$

This result is derived without any particular specification of either the value of the supersonic speed of the aerofoil or the particular distribution of the basic flow field v_i, provided that it is steady with finite dimensions in the plane in which the aerofoil moves. It can be seen from (4.7) that the scattered sound energy is independent of the Mach number of the supersonic aerofoil. For our uniform cylindrical flow, we have

$$v_3(\boldsymbol{x}) = -u_0 H(a^2 - x_\alpha^2). \tag{4.8}$$

Hence, (4.7) becomes

$$E_a = \frac{1}{2\pi}\rho_0 u_0^2 \int_{x_\alpha} \int_{y_\alpha} \frac{H(a^2 - x_\alpha^2)\, H(a^2 - y_\alpha^2)}{|y_\alpha - x_\alpha|} \mathrm{d}^2 y_\alpha \, \mathrm{d}^2 x_\alpha. \tag{4.9}$$

The x_α integral can be carried out immeditely (e.g. Ffowcs Williams & Lovely 1975),

$$\int_{x_\alpha} \frac{H(a^2 - x_\alpha^2)}{|y_\alpha - x_\alpha|} \mathrm{d}^2 x_\alpha = 4a\mathscr{E}\left(\frac{|y_\alpha|}{a}\right), \tag{4.10}$$

where $\mathscr{E}(z)$ is the complete elliptic integral of the second kind. Thus, (4.9) yields

$$E_a = \frac{2a\rho_0 u_0^2}{\pi} \int_{y_\alpha} \mathscr{E}\left(\frac{|y_\alpha|}{a}\right) H(a^2 - y_\alpha^2) \, \mathrm{d}^2 y_\alpha.$$

Changing the integration variables to polar coordinates and using the formulae (8.112) and (6.132) given by Gradshteyn & Ryzhik (1980), we find that

$$E_a = \tfrac{8}{3}\rho_0 u_0^2 a^3. \tag{4.11}$$

This is the sound energy scattered by the semi-infinite aerofoil which is only related to the parameters of the cylindrical jet flow and is independent of the supersonic aerofoil speed. This result, derived through arguments of energy conservation, can also be obtained directly from the far-field acoustic motions, which we do next, following suggestions by H. Levine in a private communication (also see Levine 1987). We start with the far-field acoustic pressure perturbations that can be found from (2.3) by approximating $1/|\boldsymbol{y}-\boldsymbol{x}|$ by $1/|\boldsymbol{x}|$ and $|\boldsymbol{y}-\boldsymbol{x}|$ by $|\boldsymbol{x}|-y_\alpha \hat{x}_\alpha$. Thus we have

$$p \sim \frac{\rho_0 u_0 cM}{2\pi|\boldsymbol{x}|}\int_{y_\alpha} H(a^2-y_\alpha^2)\,\delta(cMt-y_1-M|\boldsymbol{x}|+M\hat{x}_\alpha y_\alpha)\,\mathrm{d}^2y_\alpha,$$

$$= \frac{\rho_0 u_0 cM}{(2\pi)^2|\boldsymbol{x}|}\int_{y_\alpha}\int_k H(a^2-y_\alpha^2)\,\mathrm{e}^{\mathrm{i}k(cMt-y_1-M|\boldsymbol{x}|+M\hat{x}_\alpha y_\alpha)}\,\mathrm{d}^2y_\alpha\,\mathrm{d}k.$$

The total acoustic energy can be found by integrating the square of this result, divided by $\rho_0 c$, which gives the far-field energy flux in the radial direction, over a spherical surface of large radius $|\boldsymbol{x}|$ from time $t\to-\infty$ to $t\to+\infty$. This yields the result for the sound energy E_a,

$$E_a = \frac{2\rho_0 u_0^2 M}{(2\pi)^3}\int H(a^2-y_\alpha^2)\,H(a^2-z_\alpha^2)\,\mathrm{e}^{\mathrm{i}k[M\hat{x}_\alpha(y_\alpha-z_\alpha)-(y_1-z_1)]}\sin\theta\,\mathrm{d}\theta\,\mathrm{d}\phi\,\mathrm{d}k\,\mathrm{d}^2y_\alpha\,\mathrm{d}^2z_\alpha, \tag{4.12}$$

where the θ-integral is from 0 to $\frac{1}{2}\pi$ and that with respect to ϕ from 0 to 2π. Other integrals are all performed from $-\infty$ to $+\infty$. Now we can carry out the ϕ-integral with the result expressed in terms of a Bessel function which can then be integrated with respect to θ, according to formula (6.554) of Gradshteyn & Ryzhik's (1980), to give

$$\int_0^{2\pi}\int_0^{\pi/2}\mathrm{e}^{\mathrm{i}kM\hat{x}_\alpha(y_\alpha-z_\alpha)}\sin\theta\,\mathrm{d}\theta\,\mathrm{d}\phi = 2\pi\frac{\sin(kM|y_\alpha-z_\alpha|)}{kM|y_\alpha-z|}.$$

Substituting this into (4.12), and performing the k-integral according to

$$\int_0^\infty \frac{\sin(\eta Z)}{Z}\mathrm{d}Z = \tfrac{1}{2}\pi\,\mathrm{sgn}(\eta),$$

with sgn denoting the sign function, we find that

$$E_a = \frac{\rho_0 u_0^2}{4\pi}\int_{y_\alpha}\int_{z_\alpha}\left[\mathrm{sgn}\left(|y_\alpha-z_\alpha|+\frac{y_1-z_1}{M}\right)+\mathrm{sgn}\left(|y_\alpha-z_\alpha|-\frac{y_1-z_1}{M}\right)\right]$$

$$\times\frac{H(a^2-y_\alpha^2)\,H(a^2-z_\alpha^2)}{|y_\alpha-z_\alpha|}\mathrm{d}^2y_\alpha\,\mathrm{d}^2z_\alpha.$$

Since the Mach number M is larger than one, the arguments of both the two sign functions in the integrand are always positive. Hence the quantity enclosed in the square brackets is identically equal to 2. This result is then seen to be exactly the same as (4.9), and hence (4.11), the result derived through energy conservation arguments. The agreement of the two calculations also gives evidence that the

supersonic leading edge is indeed dragless, because the far-field calculation does not involve any assumption at the leading edge, but gives the same result as that of the energy conservation arguments which presume a dragless leading edge.

5. The trailing-edge problem

Now, we consider the reciprocal problem of that discussed in the previous sections, namely a semi-infinite plane with a trailing edge moving supersonically in the positive-x_1 direction. Though the geometry of the trailing-edge problem is 'reciprocal' to that of the leading edge, the solutions for the two situations are quite different. Actually, the supersonic-trailing-edge aerofoil does not scatter any sound. It does not affect the near-field motions either. This is evident from Kirchhoff's theorem (Dowling & Ffowcs Williams 1983) that expresses the pressure perturbations in the field in terms the pressure fluctuations on the plane $x_3 = 0$, in which the trailing edge aerofoil lies, namely

$$p(\boldsymbol{x}, t) = \frac{-1}{2\pi} \frac{\partial}{\partial x_3} \int_{y_\alpha} \left[\frac{p(\boldsymbol{y}, \tau)}{|\boldsymbol{y}-\boldsymbol{x}|}\right] \mathrm{d}^2 y_\alpha, \tag{5.1}$$

where τ is the retarded time $t-|\boldsymbol{y}-\boldsymbol{x}|/c$ and the integrand is to be evaluated at $y_3 = 0$. Since the trailing edge moves supersonically, the unsteady disturbances caused by the trailing edge, if there are any, will all be confined to the region behind the trailing edge. The motions ahead of it (on the semi-infinite aerofoil surface in particular) are then steady and the unsteady pressures $p(\boldsymbol{y}, \tau)$ vanish there. Behind the trailing edge on the plane $y_3 = 0$, $p(\boldsymbol{y}, \tau)$ is also zero owing to the symmetrical geometry. Hence we have

$$p(\boldsymbol{y}, \tau) \equiv 0 \quad \text{on } y_3 = 0 \quad \text{for any } y_\alpha.$$

The equation (5.1) thus yields that the pressure fluctuations caused by the trailing edge are identically zero, no sound being scattered. It is also clear that the trailing edge has no effect on the near-field kinetic motions either, because the total kinetic energy contained in the field is unchanged during the passage of the trailing-edge aerofoil. The total flow, being the cylindrical jet flow supplemented by the steady potential flow (4.3) that is built up by the semi-infinite trailing edge aerofoil at time $t \to -\infty$, is unchanged during the whole process.

In this case, there is no need to apply the Kutta condition at the sharp trailing edge that moves supersonically, because there is no unsteady load there. For finite aerofoils of large chord, this may also be the case, because the trailing and the leading edge in this case are likely to be energetically decoupled. If the chord is sufficiently large, the unsteady field produced by the leading edge may become so weak, owing to spherical spreading, before it reaches the trailing edge that its load at the trailing edge has no significant influence on the flow. The flow through which the trailing edge moves is then essentially the steady potential flow built up a long time ago. In other words, the trailing edge of a sufficiently large aerofoil of supersonic speed behaves in the same way as that of a semi-infinite plane.

For aerofoils of small or moderate chord, the unsteady field caused by the leading edge may induce a non-negligible load at the sharp trailing edge, the flow there behaving singularly. While the imposing of a Kutta condition at the trailing edge, which involves vortex shedding behind it, may still be a possible way to avoid the unphysical singularities at the sharp edge, as in subsonic situations (Crighton 1985), the generation of shock waves, which is the main characteristic of supersonic flows,

is a better alternative possibility to render the flow finite there. In the latter case, the unsteady load at the trailing edge, predicted by inviscid shock-free theories, would in real flows be cancelled by shock-wave discontinuities. No Kutta condition would then be needed. In general, we believe that both the production of vortices and the generation of shock waves are possible for rendering the flow field finite at the trailing edge in supersonic flows. It is reasonable to conjecture that there is a competition between these two mechanisms, their relative importance depending on how easily the two processes can take place in a particular flow. In other words, the relative importance of the typical Reynolds number and the Mach number of the flow decides the degree of predominance of either of the two mechanisms. In aeroacoustics, the typical Reynolds number is usually very high and compressive motions are the main characteristic of supersonic flows. Hence, the generation of shock waves may be a much easier process to affect than the production of vortices. This gives grounds for suggesting that it may not be necessary to impose a Kutta condition at the trailing edge for supersonic air flows, in sharp contrast with subsonic flows where vortex shedding is the *only* way to cancel the singularity at the trailing edge.

6. A piston source model for energy calculation

It can be noticed that the basic equations and the boundary conditions for the induced velocity potential φ and the pressure fluctuation p in the flow–aerofoil interaction problem are identical to those in the problem where there is *no* jet flow but a piston source of constant velocity u_0 is prescribed on the aerofoil surface within the region $|x_\alpha| < a$. Since the pressure perturbations are identical for both problems, the acoustic effects must be the same for the two situations; the sound energy radiated to infinity must be the same. The energy scattering processes are, however, different in the two cases. In this section, we establish the equivalence of the two problems when evaluating the acoustic radiation and, also, identify their differences concerning the processes of energy conversion.

Let us consider the leading-edge problem. Since there is no jet flow, the whole field at time $t \to -\infty$ when the aerofoil is far upstream is motionless and the total energy is zero. At time $t \to +\infty$ when the aerofoil is far downstream, the total kinetic energy in the field is determined by the piston-induced velocity potential that satisfies the Laplace equation $\nabla^2\varphi = 0$ and the boundary condition

$$\frac{\partial\varphi}{\partial x_3} = u_0 H(a^2 - x_\alpha^2) \quad \text{on } x_3 = 0. \tag{6.1}$$

This gives

$$\varphi = \frac{u_0}{2\pi}\int_{y_\alpha} \frac{H(a^2-y_\alpha^2)}{|\boldsymbol{y}-\boldsymbol{x}|}\,\mathrm{d}^2 y_\alpha. \tag{6.2}$$

The kinetic energy E_k can be calculated according to

$$E_\mathrm{k} = \int \tfrac{1}{2}\rho_0(\boldsymbol{\nabla}\varphi)^2\,\mathrm{d}^3\boldsymbol{x} = \tfrac{1}{2}\rho_0\int \boldsymbol{\nabla}(\varphi\boldsymbol{\nabla}\varphi)\,\mathrm{d}^3\boldsymbol{x},$$

where we have used $\nabla^2\varphi = 0$ to derive the last step. Applying the divergence theorem to the volume integral with a result expressed in terms of φ and $\partial\varphi/\partial x_3$ on $x_3 = 0$, which are given respectively by (6.1) and (6.2), we find that

$$E_\mathrm{k} = \frac{\rho_0 u_0^2}{2\pi}\int_{x_\alpha}\int_{y_\alpha} \frac{H(a^2-x_\alpha^2)H(a^2-y_\alpha^2)}{|\boldsymbol{y}-\boldsymbol{x}|}\,\mathrm{d}^2 x_\alpha\,\mathrm{d}^2 y_\alpha = \tfrac{8}{3}\rho_0 u_0^2 a^3. \tag{6.3}$$

This is the near-field energy produced by the piston source, which remains in the field long after the passage of the leading edge. The acoustic energy is then equal to the difference between the total energy radiated by the piston source and the near-field energy (6.3). The former can be calculated by integrating the energy flux over an infinite plane control surface just above the coordinate plane $x_3 = 0$. The expression for the pressure fluctuations on this control surface can be chosen as (2.3) with $x_3 \to 0$, which is a convenient form for evaluating the energy, and the velocity on this surface is given by (6.1) on the aerofoil and vanishes otherwise. Hence, the energy flux on the control surface is

$$\frac{\rho_0 u_0^2 cM}{2\pi} H(a^2-x_\alpha^2)\, H(cMt-x_1) \int_{y_a} \frac{H(a^2-y_\alpha^2)}{|y_\alpha - x_\alpha|} \delta(cMt - M|y_\alpha - x_\alpha| - y_1)\, \mathrm{d}^2 y_\alpha. \quad (6.4)$$

The total energy produced by the piston source is twice the result obtained by integrating this over time t and space x_α, being twice because the same amount of energy is radiated into the lower half-space. The t-integral can be performed by utilizing the δ-function, to yield the result

$$E = \frac{\rho_0 u_0^2}{\pi} \int_{y_a} \int_{x_a} \frac{H(a^2-y_\alpha^2)\, H(a^2-x_\alpha^2)}{|y_\alpha - x_\alpha|} \mathrm{d}^2 y_\alpha\, \mathrm{d}^2 x_\alpha = \tfrac{16}{3} \rho_0 u_0^2 a^3. \quad (6.5)$$

It is now clear that the piston source produces the same amount of acoustic energy as that scattered from the jet flow by a semi-infinite aerofoil, because the difference between (6.5) and (6.3)

$$E - E_{\mathrm{k}} = \tfrac{8}{3} \rho_0 u_0^2 a^3$$

is exactly equal to (4.11), the sound energy from the flow–aerofoil interaction. From the foregoing analysis, we see that the total energy (6.5), produced by the piston source, is equally shared between the near-field steady potential motions and the far-field outward-travelling acoustic wave motions. This kind of equipartition of energy has been observed previously in a variety of impact-sound problems (see, for example, Taylor 1942 and Hill 1986). It is also clear that, though the same amount of energy is radiated to the far field as sound in both the flow–aerofoil interaction problem and the piston source problem, the processes of energy conversion are quite different, the near-field motions being different for the two cases. For the flow–aerofoil problem, no energy is produced from the aerofoil surface because the energy flux on the plane $x_3 = 0$ is identically zero, and the sound energy radiated to infinity is all scattered from the cylindrical steady jet flow, while in the piston source problem, both the acoustic radiation and the near-field kinetic energy come from the energy produced at the aerofoil surface because the piston source in this case does work on the fluid.

7. Energy scattered by a finite-chord aerofoil

In practice, aerofoils have finite chord and it is obviously of interest to see whether the finiteness of the aerofoils can significantly affect the generated sound. We consider an aerofoil of finite chord $2b$ that moves supersonically in the plane $x_3 = 0$. Since the disturbances caused by the trailing edge of the supersonic aerofoil cannot affect the field ahead of it, the pressure fluctuations on the finite aerofoil surface are precisely the same as those on a semi-infinite aerofoil, which is given by (2.3) with

$x_3 = 0$. Because the pressure fluctuations vanish elsewhere in the plane $x_3 = 0$ owing to symmetry, (2.3) can be utilized to find the pressure perturbations in the field according to Kirchhoff's theorem (5.1), and hence, the acoustic energy radiated to infinity. The energy can also be calculated in the piston source model through the evaluation of the energy across the plane control surface just above the coordinate plane $x_3 = 0$. In this event, the velocity distribution on the aerofoil has the same specification as that in the semi-infinite case, both being determined according to the vanishing normal velocity boundary condition; it is given by (6.1) on the finite aerofoil surface but vanishes elsewhere. Behind the trailing edge, the velocity distribution is unknown, but this does not affect the energy calculation, because the pressure fluctuations there always vanish owing to symmetry, and so too does the energy flux. Hence the energy flux in the plane $x_3 = 0$ for this finite-chord situation is still given by (6.4), provided we replace $H(cMt-x_1)$ by

$$H(cMt-x_1)-H(cMt-x_1-2b).$$

Integrating the result over time t and space x_α, we derive an expression

$$E_b = \frac{\rho_0 u_0^2}{\pi}\int_{y_\alpha}\int_{x_\alpha}\frac{H(a^2-y_\alpha^2)\,H(a^2-x_\alpha^2)}{|y_\alpha-x_\alpha|}H[2b-(y_1-x_1)-M|y_\alpha-x_\alpha|]\,\mathrm{d}^2y_\alpha\,\mathrm{d}^2x_\alpha, \quad (7.1)$$

where we have multiplied the result by two to take account of the energy into the lower half-space, so that E_b is the total energy produced by the aerofoil. The integrals in (7.1) can be evaluated by changing the integration variables x_α and y_α into polar coordinates according to

$$\begin{cases} x_1-y_1 = k\cos\alpha, \\ x_2-y_2 = k\sin\alpha, \end{cases} \quad \begin{cases} y_1 = \lambda\cos\beta, \\ y_2 = \lambda\sin\beta, \end{cases}$$

which transfer (7.1) to

$$E_b = \frac{\rho_0 u_0^2}{2\pi}\int H[a^2-k^2-\lambda^2-2k\lambda\cos(\alpha-\beta)]\,H[2b-k(\cos\alpha+M)]\,\lambda\,\mathrm{d}\lambda\,\mathrm{d}k\,\mathrm{d}\alpha\,\mathrm{d}\beta, \quad (7.2)$$

where both the α-integral and the β-integral are performed from 0 to 2π, the λ-integration is from 0 to a and that with respect to k along the positive k-axis. In (7.2), we can replace $\cos(\alpha-\beta)$ in the first Heaviside function by $\cos\beta$, because the β-integral is over a complete period. Thus, the α-integral and the λ-integral can be evaluated separately, by utilizing respectively the two Heaviside functions, with the results

$$\int_0^{2\pi} H[2b-k(\cos\alpha+M)]\,\mathrm{d}\alpha = 2H\left(\frac{2b}{k}-M+1\right)\left[\pi-\arccos\left(\frac{2b}{k}-M\right)H\left(1+M-\frac{2b}{k}\right)\right],$$

and

$$\int_0^a H(a^2-k^2-\lambda^2-2k\lambda\cos\beta)\,\lambda\,\mathrm{d}\lambda = \tfrac{1}{2}a^2[H(a-\lambda_-)-H(a-\lambda_+)] + \tfrac{1}{2}\lambda_+^2 H(\lambda_+)H(a-\lambda_+)-\tfrac{1}{2}\lambda_-^2 H(\lambda_-)H(a-\lambda_-),$$

where

$$\lambda_\pm = -k\cos\beta\pm(a^2-k^2\sin^2\beta)^{\frac{1}{2}}.$$

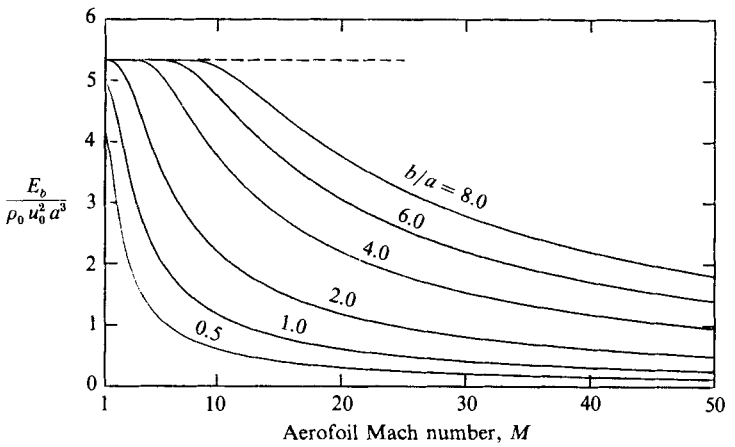

FIGURE 9. Energy scattered by aerofoils of finite chord. The dashed line indicates the energy from a semi-infinite aerofoil.

On substituting these results into (7.2) and carrying out the β-integral, we find that

$$E_b = \frac{\rho_0 u_0^2}{2\pi}\int_0^{2a} H\left(\frac{2b}{M-1}-k\right)\left[4a^2\arccos\left(\frac{k}{2a}\right)-k(4a^2-k^2)^{\frac{1}{2}}\right] \times\left[\pi - H\left(k-\frac{2b}{M+1}\right)\arccos\left(\frac{2b}{k}-M\right)\right]\mathrm{d}k.$$

This can be further calculated as

$$E_b = \begin{cases} \frac{16}{3}\rho_0 u_0^2 a^3 & \text{when } \dfrac{a}{b} < \dfrac{1}{M+1} < \dfrac{1}{M-1}, \\ \frac{16}{3}\rho_0 u_0^2 a^3\left[1+\dfrac{b}{2\pi a}f(1)\right] & \text{when } \dfrac{1}{M+1} < \dfrac{a}{b} < \dfrac{1}{M-1}, \\ \frac{16}{3}\rho_0 u_0^2 a^3\left[1+\dfrac{b}{2\pi a}f\left(\dfrac{b}{a(M-1)}\right)\right] & \text{when } \dfrac{1}{M+1} < \dfrac{1}{M-1} < \dfrac{a}{b}, \end{cases} \tag{7.3}$$

where $f(z)$ is a complicated combination of elementary functions and elliptic functions, but it can also be expressed by a simple integral as

$$f(z) = \int^z \frac{3\eta\arccos\eta-(2+\eta^2)(1-\eta^2)^{\frac{1}{2}}}{\eta(2M\eta b/a-b^2/a^2-(M^2-1)\eta^2)^{\frac{1}{2}}}\mathrm{d}\eta,$$

with the lower limit of integration given by $b/a(M+1)$.

These results are shown in figures 9 and 10, where the energy produced by the finite-chord aerofoil is plotted as a function of the aerofoil Mach number M in figure 9 and as a function of the parameter b/a in figure 10, which is the ratio of the aerofoil chord to the diameter of the cylindrical flow. Apparently, the upper bound of the radiated energy is that of a semi-infinite aerofoil, namely the result (6.5), which is illustrated by the dashed line. This maximum energy is achieved, not as a limiting process as the aerofoil chord tends to infinity, but at a condition $b > a(M+1)$, as indicated by (7.3). For aerofoils with chord larger than $2a(M+1)$, the radiated energy is independent of the aerofoil Mach number just as a semi-infinite aerofoil is.

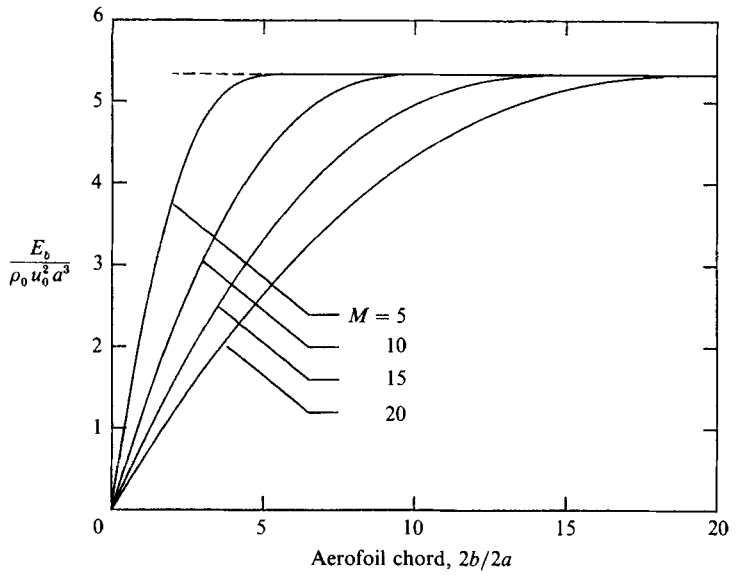

FIGURE 10. The scattered energy as a function of the aerofoil chord. Note the rapid transition from the linear increase at small values of b/a to the constant value $\frac{16}{3}$, namely, the energy for a semi-infinite plane.

As analysed in §5, the supersonic trailing edge in this case of large-chord aerofoil behaves in the same way as that of the semi-infinite plane, and has no influence on the flow field. This energy is then equally shared between the far-field acoustic waves and the near-field steady potential motions.

For a fixed aerofoil chord, the radiated energy decreases as the Mach number M increases, indicating that the faster the supersonic aerofoil moves, the quieter the sound field will be. The decrease of E_b can be shown to be $1/M$ at high values of M. It is straightforward to demonstrate this by evaluating (7.1) in the limiting case of $M \gg 1$. The x_α integral can be performed, in this event, as

$$\int_0^{2\pi} [S_1(\alpha) H(S_0 - S_1) + S_0(\alpha) H(S_1 - S_0)] \, \mathrm{d}\alpha, \tag{7.4}$$

where $$S_1(\alpha) = [a^2 - y_\alpha^2 \sin^2(\alpha - \beta)]^{\frac{1}{2}} - |y_\alpha| \cos(\alpha - \beta),$$

and $$S_0(\alpha) = \frac{2b}{M + \cos\alpha}, \quad \beta = \arctan(y_2/y_1).$$

Apparently, $H(S_0 - S_1)$ vanishes and $H(S_1 - S_0) \to 1$ in the case of $M \gg 1$. Hence, (7.4) reduces to

$$\int_0^{2\pi} \frac{2b}{M + \cos\alpha} \mathrm{d}\alpha = \frac{4\pi b}{(M^2 - 1)^{\frac{1}{2}}}. \tag{7.5}$$

Equations (7.5) and (7.1) then yield that, for $M \gg 1$,

$$E_b \sim \frac{2\pi \rho_0 u_0^2 a^2 b}{M}. \tag{7.6}$$

This result clearly reveals a $1/M$-dependence of the radiated energy; it decreases as the supersonic aerofoil speed increases, mainly because of the reducing duration of

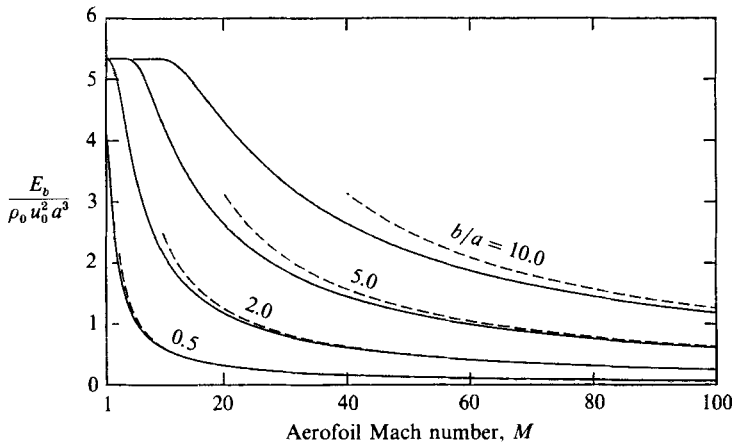

FIGURE 11. The scattered energy by a finite-chord aerofoil decreases as $1/M$ at high supersonic aerofoil speeds: ——, exact calculation; – – –, asymptotic result.

the pressure pulse at high supersonic speed. The asymptotic solution (7.6) is compared, in figure 11, with the exact calculations of (7.3). The result (7.6) also predicts a linear relation between the energy and the chord of the aerofoil. The linear increase of sound with the dimension of the aerofoil is true only for the case of high supersonic speed and moderate chord; for fixed M and very large b, (7.4) reduces to (4.10) instead of (7.5), because $H(S_0-S_1)$ would then be equal to unity and $H(S_1-S_0)$ vanishes, and the energy is given in this case by the first line of (7.3). The dependence of the radiated energy on the dimension of the aerofoil is illustrated in figure 10; E_b increases linearly with the aerofoil chord at small values of b/a, but rapidly approaches the value $16\rho_0 u_0^2 a^3/3$, that is, the value for a semi-infinite plane, as the ratio b/a increases.

8. Conclusions

We have examined a flow–aerofoil interaction problem. The sound generated by a semi-infinite plane with a leading edge moving supersonically through and interrupting a uniform cylindrical flow has been found exactly. The generated sound takes the form of a pressure pulse of finite duration. In directions other than the Mach-wave direction, the pressure pulse is switched on and off at zero amplitude, and has a maximum in the middle, which decreases, owing to spherical spreading, inversely in proportion to the distance that the pulse travels. Along the Mach angle, it has been found that the pulse has sharp faces (both front and rear) and constant amplitude; it reaches distant observers without attenuation according to linear theory. It is the noisiest sound from the flow–aerofoil interaction and is, we believe, likely to be one of the most important aspects concerning the noise of aircraft using supersonic propellers.

The energy radiated to infinity has been calculated explicitly. For a semi-infinite aerofoil, the sound is scattered from the uniform jet flow; the loss of kinetic energy of the jet flow during the whole interruption process has been shown to be precisely equal to the energy radiated as sound to infinity. The scattered acoustic energy has been shown to be independent of the Mach number at which the supersonic semi-infinite plane moves. By calculating the sound energy radiated to infinity and

considering the conservation of energy, it has been demonstrated that the supersonically moving aerofoil does not experience any force whose work might affect the sound generation process.

The trailing-edge problem has also been considered. For a semi-infinite aerofoil, it has been shown that the supersonic trailing edge has no effect on the flow at all; it can neither radiate sound, nor alter the near-field motions. This has been shown to be also true for finite aerofoils of large chord, in particular, for aerofoils of chord larger than the diameter of the cylindrical flow times $M+1$. At high supersonic speeds, it has been demonstrated that finite-chord aerofoils radiate energy that decreases inversely as the Mach number of the aerofoil increases; the higher the speed, the quieter will be the sound generated as a result of flow scattering by a finite-chord supersonic aerofoil.

Y. P. Guo gratefully acknowledges the encouragement and financial support provided by Rolls Royce p.l.c. The authors would also like to thank Professor R. S. Scorer for providing the photograph in figure 1.

REFERENCES

AMIET, R. K. 1986*a* Airfoil gust response and the sound produced by airfoil–vortex interaction. *J. Sound Vib.* **107**, 487–506.

AMIET, R. K. 1986*b* Intersection of a jet by an infinite span airfoil. *J. Sound Vib.* **111**, 499–503.

CANNELL, P. & FFOWCS WILLIAMS, J. E. 1973 Radiation from line vortex filaments exhausting from a two-dimensional semi-infinite duct. *J. Fluid Mech.* **58**, 65–80.

CRIGHTON, D. G. 1985 The Kutta condition in unsteady flow. *Ann. Rev. Fluid Mech.* **17**, 411–445.

DOWLING, A. P. & FFOWCS WILLIAMS, J. E. 1983 *Sound and Sources of Sound*. Ellis Horwood.

FFOWCS WILLIAMS, J. E. & LOVELY, D. J. 1975 Sound radiation into uniformly flowing fluid by compact surface vibration. *J. Fluid Mech.* **71**, 689–700.

GRADSHTEYN, I. S. & RYZHIK, I. M. 1980 *Table of Integrals, Series and Products* (corrected and enlarged edition). Academic.

HILL, D. C. 1986 Starting mechanics of an evanescent wave field. *J. Fluid Mech.* **165**, 319–333.

JEFFREYS, H. & JEFFREYS, B. 1956 *Methods of Mathematical Physics*. Cambridge University Press.

JONES, D. S. 1982 *The Theory of Generalized Functions*. Cambridge University Press.

KÁRMÁN, VON T. & SEARS, W. R. 1938 Airfoil theory for non-uniform motion. *Aeronaut. Sci.* **5**, 379–390.

LEVINE, H. 1987 Acoustic power output from moving point singularities. *J. Acoust. Soc. Am.* **81**, 1695–1702.

MILES, J. E. 1959 *The Potential Theory of Unsteady Supersonic Flow*. Cambridge University Press.

TAYLOR, G. I. 1942 The motion of a body in water when subject to a sudden impulse. In *Scientific Papers of G. I. Taylor* (ed. G. K. Batchelor), vol. 3, pp. 306–308. Cambridge University Press.

TEMPLE, G. 1953 Unsteady motions, *Modern Developments in Fluid Dynamics: High Speed Flow* (ed. L. Howarth). Clarendon.

WARD, G. N. 1955 *Linearized Theory of High Speed Flow*. Cambridge University Press.